Quarterly Reviews of Biophysics **46**, 4 (2013), pp. 323–348. © Cambridge University Press 2013
doi:10.1017/S0033583513000073 Printed in the United States of America

Single-molecule views on homologous recombination

Andrea Candelli[1], Mauro Modesti[2,3,4,5], Erwin J. G. Peterman[1] and Gijs J. L. Wuite[1]*

[1] LaserLaB and Department of Physics and Astronomy, VU University Amsterdam, Amsterdam, The Netherlands
[2] Centre de Recherche en Cancérologie de Marseille, CNRS, UMR7258, Marseille F-13009, France
[3] Inserm U1068, Marseille F-13009, France
[4] Institut Paoli-Calmettes, Marseille F-13009, France
[5] Aix-Marseille Université, Marseille F-13284, France

Abstract. All organisms need homologous recombination (HR) to repair DNA double-strand breaks. Defects in recombination are linked to genetic instability and to elevated risks in developing cancers. The central catalyst of HR is a nucleoprotein filament, consisting of recombinase proteins (human RAD51 or bacterial RecA) bound around single-stranded DNA. Over the last two decades, single-molecule techniques have provided substantial new insights into the dynamics of homologous recombination. Here, we survey important recent developments in this field of research and provide an outlook on future developments.

1. Introduction 323
1.1. Double-stranded DNA (dsDNA) breaks and homologous recombination (HR) 323
1.2. Structure and conformations of human RAD51 and E. coli RecA 325

2. Single-molecule techniques for the study of DNA–protein interactions 326

3. Single-molecule experiments 329
3.1. Assembly of the NPF 329
3.2. Conformational transitions of the NPF 334
3.3. Searching for a needle in the haystack 336
3.4. Strand-exchange at the single-molecule level 339
3.5. RAD51 disassembly from DNA 342

4. Conclusions and outlook 344

5. Acknowledgement 345

6. References 345

1. Introduction

1.1 Double-stranded DNA (dsDNA) breaks and homologous recombination (HR)

Ultimately, the biological essence of life consists in the accurate transmission of genetic information from one generation to the next. Preserving genome integrity against DNA damages is therefore crucial for living organisms. Among the different types of DNA damage encountered,

* Author for Correspondence: G. J. L. Wuite, LaserLaB and Department of Physics and Astronomy, VU University Amsterdam, Amsterdam, The Netherlands. gwuite@nat.vu.nl

https://doi.org/10.1017/S0033583513000073 Published online by Cambridge University Press

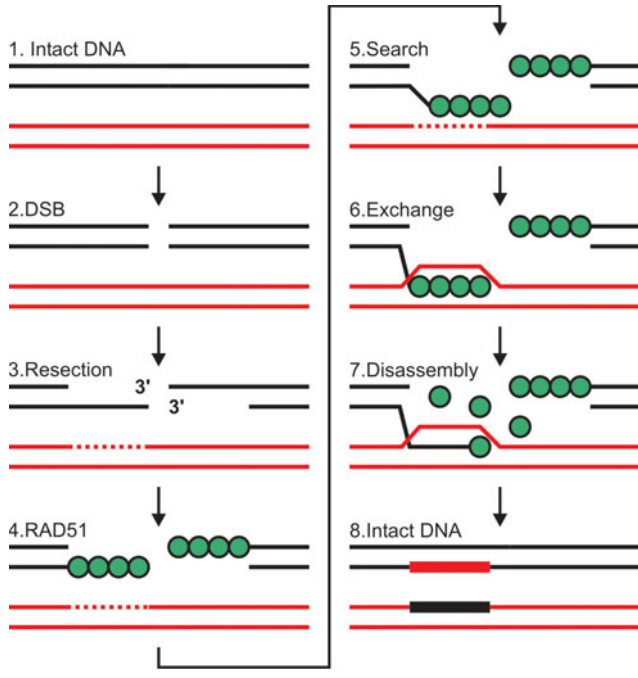


Fig. 1. HR pathway. [1] Two intact identical copies of the genome in somatic cells in S and G2 phases. [2] Occurrence of a DNA double-stranded break (DSB). [3] End-resection creates a 3′ ssDNA tail. [4] RAD51, assisted by recombinase mediators assembles in form of filaments on ssDNA. [5] Homology search: the NPF needs to find the homologous DNA sequence among a large abundance of non-complementary sequence. End of the pre-synaptic phase. [6] Sequence homology is found and a stable complex is formed. During this process, one of the strands of the target DNA (red) is displaced and interacts with the secondary-binding site of the recombinase filament. End of synaptic phase. [7] RAD51 unbind from the DNA duplex, triggered by ATP hydrolysis (Start of post-synaptic phase). [8] The cross-over structure is resolved by specialized enzymes and genomic integrity is re-established.

DNA double-strand breaks (DSB) pose a serious threat to cell survival. If left unrepaired they can lead to chromosomal fragmentation and genomic rearrangements, a hallmark of many cancers (Hoeijmakers, 2001; Inoue & Lupski, 2002). Various chemicals or environmental agents such as ionizing radiations can cause DSBs. In addition, they can also form endogenously through the action of reactive oxygen species generated as by-products of cellular metabolism or during genetically programmed genomic rearrangements as during meiotic recombination. One of the fundamental cellular strategies to repair DSBs is HR. In somatic cells, HR is active during the S and G2 phase of the cell cycle (Heyer *et al.* 2010), when sister chromatids are available to serve as a template for the recovery of the genetic information. HR is a highly regulated and accurate process, which is able to restore chromosome integrity without losing genetic information (San Filippo *et al.* 2008; Wyman & Kanaar, 2006). The basic scheme of HR is similar across all domains of life and can be divided in three stages (Heyer *et al.* 2010; San Filippo *et al.* 2008): pre-synapsis, synapsis and post-synapsis (Fig. 1). In pre-synapsis, the broken DNA ends are processed by a specialized set of proteins (end-resection machinery) that create long 3′-tailed single-stranded DNA (ssDNA) overhangs. ssDNA-binding proteins, such as Replication Protein A (RPA) in humans, immediately cover the exposed ssDNA to protect it from degradation (Wold, 1997). Next, recombinase proteins (RAD51 in eukaryotes, RecA in *Escherichia coli*),

https://doi.org/10.1017/S0033583513000073 Published online by Cambridge University Press

assisted by recombinase mediators (in human: tumour suppressor protein BRCA2 and the RAD51 paralogues including RAD51B, RAD51C, RAD51D, XRCC2 and XRCC3), displace RPA and form nucleoprotein filaments (NPFs) on the ssDNA overhangs (Holloman, 2011; Jensen *et al.* 2010; Liu *et al.* 2010). The NPF, in turn, is able to find (homology search/recognition) and pair (strand exchange) with a homologous section of a dsDNA template. ATP-hydrolysis triggers RAD51 disassembly, creating a joint-structure that serves as priming site for DNA synthesis and recovery of the genetic information. Finally, the joint intermediates are resolved and ligated, restoring the integrity of the broken DNA molecule.

Malfunctions in DNA repair processes can cause chromosome instability (Hoeijmakers, 2001), one of the causes of cancer formation (Negrini *et al.* 2010). In addition, mutations in HR genes have been linked to various forms of hereditary diseases (Hoeijmakers, 2001). For example, biochemical and genetic studies pose the process of nucleoprotein-filament formation at the centre of a complex network of mediators that include important tumour-suppressor proteins such as BRCA2 and various helicases (BLM, FANCJ, RecQ5), which are implicated in different forms of tumours (Cerbinskaite *et al.* 2012; Hoeijmakers, 2001; McKinnon & Caldecott, 2007). Understanding the dynamics and the regulation of the RAD51 NPF is therefore not only important for understanding HR mechanisms but can also provide insights in the molecular causes underlying carcinogenesis.

1.2 Structure and conformations of human RAD51 and E. coli RecA

Recombinase proteins RAD51 (human) and RecA (*E. coli*) are considered to be the central HR catalysts, since they are involved in the core step of the recombination process, the exchange of DNA strands between homologous sections of the chromosomes (Benson *et al.* 1994). RecA and RAD51 are structurally and functionally similar, but are in certain respects remarkably different. Both RAD51 and RecA are globular proteins with a molecular weight of $\sim$38 kDa and DNA-stimulated ATPase activity (Baumann *et al.* 1996; Tombline & Fishel, 2002). These recombinase proteins form right-handed helical filaments around ssDNA and dsDNA (Kowalczykowski *et al.* 1994; Yu *et al.* 2001). Human RAD51 and E. coli RecA bind to both ssDNA and dsDNA in the presence of ATP with a stoichiometry of one monomer per three nucleotides (Benson *et al.* 1994; Prvost & Takahashi, 2003; Tombline & Fishel, 2002), resulting in a helical structure with approximately six proteins per helical turn (Yu *et al.* 2001). X-ray crystallography and electron microscopy studies have provided snapshots of the dynamic rearrangements of NPFs, demonstrating the existence of distinct conformations depending on nucleotide bound to the ATPase active site, that is located at the monomer–monomer interface within the recombinase filament (Chen *et al.* 2008; Conway *et al.* 2004; Reymer *et al.* 2009). In the case of human RAD51, NPFs formed in the presence of ssDNA and ATP, exhibit an extended conformation, characterized by a pitch of 9.9 nm (Yu *et al.* 2001), which results in an average axial rise per base of 0.51 nm, approximately 50% longer than B-form dsDNA (0.34 nm). RAD51-ssDNA filaments assembled in the presence of ADP or ATP-γ-S, are significantly shorter, with a helical pitch of only 7.6 nm (Yu *et al.* 2001) (average axial rise per base is 0.39 nm). The structural difference between these two conformations consists in the position of the N-terminal domain, which undergoes a rotation from the extended ATP-bound state to the compressed ADP-bound form (Yu *et al.* 2001). RecA, the bacterial homologue of RAD51, displays similar structural properties, also showing two different conformations with elongated or compressed pitch (10 *versus* 8 nm) according to the nucleotide bound (ATP *versus* ADP) (Prvost & Takahashi, 2003). One of the differences between

https://doi.org/10.1017/S0033583513000073 Published online by Cambridge University Press

RAD51 and RecA is the impact the nucleotide bound at the monomer–monomer interface has with respect to the filament structure and function. The non-hydrolyzable ATP analogue ATP-γ-S, for example, activates strand-exchange activity in RecA filaments by keeping them in the extended conformation. In contrast, RAD51 filaments formed in the presence of ATP-γ-S are in a compressed conformation. For RecA the two conformations display very different biochemical functions: ATP-bound-extended filaments are able to perform strand exchange with high efficiency, whereas the ADP-bound-compressed form is less active, and might represent an intermediate state before disassembly (Prvost & Takahashi, 2003). The same is expected for RAD51 (Bugreev & Mazin, 2004) yet it is not completely settled.

A recent X-ray crystallography study on RecA (Chen *et al.* 2008) has revealed important insights on how ssDNA and dsDNA are engaged by the recombinase filament. In the RecA–ssDNA complex the average base-to-base distance is 0.51 nm, 50% longer than in the B-DNA form (0.34 nm). The inter-base distance, however, is not uniform throughout the filament. Every RecA monomers binds three bases. Within the triplet, base stacking is observed between two bases, resulting in a B-DNA-like conformation, with a slightly elongated axial rise of 0.42 nm. The last base of one triplet and the first one of the next shows a significant local stretching (0.78 nm) and no base stacking interactions. In addition, RecA has a secondary binding site, whose role in strand exchange is still unclear. This secondary binding site binds ssDNA with higher affinity than dsDNA. Its possible role is therefore to interact with the ssDNA strand that is displaced during strand exchange (Howard-Flanders *et al.* 1984; Mazin & Kowalczykowski, 1996, 1998) and stabilize the nascent strand exchange complex.

Although these structural studies provide insights in HR with atomic resolution, only static snapshots of some of the reaction intermediates are available. Isolating, addressing and quantifying the dynamic features of this complex biophysical process are fundamental to obtain a detailed knowledge of the HR process. Over the past two decades, DNA–protein interaction studies have been revolutionized by the development and application of single-molecule techniques (Candelli *et al.* 2011). These approaches are very well suited for resolving the dynamics of complex and heterogeneous biological transitions. The HR process and in particular recombinase proteins (RecA and RAD51) have been under intense study using these novel methods. In this review, we will provide an overview of the methods used, highlight some of the performed experiments and present an outlook of what can be expected in the years to come.

2. Single-molecule techniques for the study of DNA–protein interactions

In the last two decades, a substantial advancement has been made to develop and apply novel technologies for providing a quantitative description of DNA–protein interactions. The field of single-molecule technologies, in particular, experienced a tremendous increase in its importance. Here, we will briefly discuss the three classes of single-molecule techniques that have been most successfully applied to study HR.

The first class is based on the mechanical manipulation of individual DNA molecules using optical (Moffitt *et al.* 2008) or magnetic tweezers (De Vlaminck & Dekker, 2012). Using these approaches, the interaction between proteins and DNA is followed by monitoring the changes in the mechanical properties of the DNA substrate, such as the contour or the persistence length (Fig. 2). In both methods, ssDNA or dsDNA needs to be attached to force transducers. In all these experiments, an individual-ssDNA or dsDNA molecule is attached from its extremities between two surfaces, one of them acting as force transducer. In magnetic and single-optical

https://doi.org/10.1017/S0033583513000073 Published online by Cambridge University Press

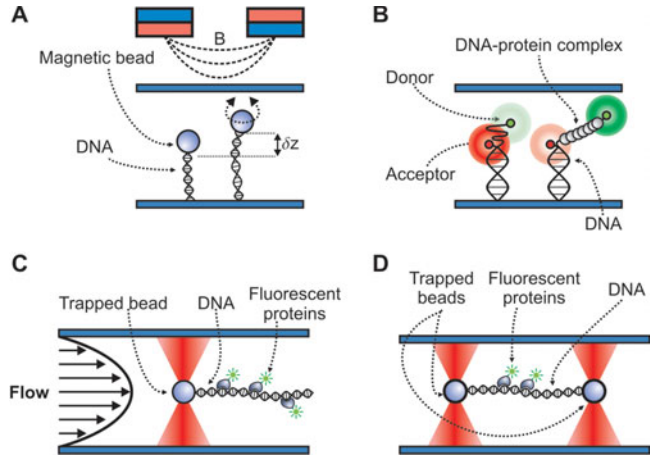


Fig. 2. Single-molecule techniques for studying homologous recombination. (*A*) Magnetic tweezers scheme for studying. A pair of magnets is used to extend and rotate a DNA molecule tethered between the glass and the paramagnetic bead. Protein binding inducing mechanical modifications of the DNA structure can be monitored in real time following the change in twist or end-to-end length of the molecule. (*B*) Single-molecule FRET spectroscopy. A duplex DNA containing a ssDNA overhang is labelled with a donor-acceptor fluorophores pair. The formation of a DNA–protein complex results in a change in distance between the FRET-pair and a concomitant reduction in FRET efficiency. (*C*) Optical tweezers combined with DNA-flow stretching and fluorescence microscopy. A DNA molecule is attached via a single-end to a optically trapped bead. The drag caused by the flow keeps the DNA in a elongated configuration and a non-uniform tension is applied along the DNA molecule. Binding and translocation of fluorescent proteins can be detected using fluorescent microscopy. (*D*) Dual-optical trapping and fluorescence microscopy. A single-DNA molecule is attached to two optically trapped beads and hold in an extended configuration, while the force applied along the DNA applied uniformly and measured with sup-pN precision. Binding and unbinding of fluorescent proteins can be resolved via fluorescence microscopy.

tweezers, the two surfaces consist of a micron-sized bead and a glass slide or a micropipette. For dual-optical tweezers the DNA molecule is directly attached to two micro-spheres. The extension of the DNA and the tension applied to it can be measured and controlled with high precision (on the nanometre scale and sub-piconewton resolution). The key difference between the two techniques is the physical nature of the bead manipulation mechanism.

In an optical tweezers instrument, the tight focus of a near-infrared laser beam generates a three-dimensional (3D) trap due to the momentum transfer from the laser light to the micro-sphere (Ashkin *et al.* 1986). In this way, transparent, μm-sized spheres can be stably held. Optical tweezers are currently capable of distinguishing mechanical changes in length of the DNA molecule with Angstrom precision (Abbondanzieri *et al.* 2005; Shaevitz *et al.* 2003) and apply forces as high as high as hundreds of piconewtons (Neuman & Block, 2004).

In a magnetic tweezers instrument, an electromagnet or permanent magnet is mounted on a motorized stage in close proximity to the sample. The DNA is attached with one end to the surface of the microscope slide and with the other end to a paramagnetic microsphere. The magnetic field acting on the magnetic dipole of the paramagnetic microsphere allows the extension and coiling of single biopolymers attached between the glass surface and the micro-sphere (Smith *et al.* 1992; Strick *et al.* 1996). Key advantages of magnetic tweezers over optical tweezers are the possibility to coil the DNA (Lipfert *et al.* 2010) and that many tethers can be followed in parallel (De Vlaminck *et al.* 2011). Recently, methods to directly measure the torque

https://doi.org/10.1017/S0033583513000073 Published online by Cambridge University Press

acting on the DNA have been devised (Lipfert *et al.* 2011). In terms of sensitivity, the capability of magnetic tweezers of achieving sub-nm resolutions has been only recently demonstrated using more sophisticated bead-imaging schemes (Kim & Saleh, 2009). Also, the forces that can be reached using magnetic tweezers are about an order of magnitude smaller than what can be achieved with optical tweezers.

In an extension of the optical and magnetic tweezers methods discussed above, several laboratories have successfully embarked on methods that allow the manipulation of two DNA molecules at the same time, in order to study (protein-mediated) interactions between the two DNA molecules. So far, an optical tweezers instrument equipped with four independently steerable optical traps has been developed and applied to study the protein-mediated bridging between different DNA molecules (Dame *et al.* 2006) and to localize individual proteins bound to DNA (Noom *et al.* 2007). More recently, this approach has been further expanded, using a combination of optical and magnetic tweezers, enabling the controlled application of torque in dual-DNA-manipulation experiments (De Vlaminck *et al.* 2012).

A second class of single-molecule approaches to study DNA–protein interactions is single-molecule fluorescence microscopy, in particular employing single-pair Förster Resonance Energy Transfer (spFRET) (Fig. 2). FRET is a photo-physical phenomenon in which two fluorescent molecules (commonly referred as the donor–acceptor pair) exchange energy through a non-radiative process (Ha *et al.* 1996). The efficiency of FRET is dependent on the nature of the two fluorophores (in particular the overlap between the fluorescence spectrum of the donor molecule and the absorption spectrum of the acceptor) and, in a highly non-linear fashion on the distance between donor and acceptor (which needs to be less than 10 nm for FRET to occur). A widely applied scheme to study DNA–protein interactions using spFRET consists in labelling the protein or the substrate of interest at a specific position with a donor–acceptor pair and monitor the change in FRET efficiency upon the progression of the biophysical interaction (McKinney *et al.* 2006; Roy *et al.* 2008) (Fig. 2). In addition, experiments and theory both validated the use of spFRET as a molecular ruler capable of resolving movements equivalent to single base pairs (Holden *et al.* 2010). spFRET has been applied successfully to helicases (Yodh *et al.* 2010), DNA polymerases (Santoso *et al.* 2010) and protein movement on ssDNA (Ha *et al.* 2012).

A third and rapidly expanding category of single-molecule approaches involves combinations of DNA manipulation and visualization using fluorescence microscopy. Examples of such methodology include fluorescence microscopy combined with DNA combing or flow stretching (Blainey *et al.* 2006). In this approach, single DNA molecules are covalently attached with one end to a functionalized glass surface and extended by the viscous drag generated by the buffer-flow. Fluorophores bound on the DNA or fluorescently labelled DNA-bound proteins, can be visualized using Total Internal Reflection Fluorescence microscopy (TIRF-M). This approach can be expanded using 'DNA curtains', a specialized patterned attachment protocol that allow multiple DNA molecules to be bound next to each other along lines perpendicular to the solvent flow, which is excellent for massive parallelization of the experiments (Gorman *et al.* 2010). Also, very recently, it has become possible to apply this method to ssDNA substrates using a dual-attachment strategy (Gibb *et al.* 2012). A limitation of surface-based assays is the vicinity of the glass surface to the DNA that can cause unwanted electrostatic interactions and the inability to control the conformation of the DNA in a dynamic way. DNA flow stretching was therefore combined to optical trapping (Quake *et al.* 1997) (Fig. 2). In this way, only a single DNA molecule can be followed at a time. The method is, however, compatible with microfluidics, allowing rapid buffer exchange, which permits fluorescence imaging in the absence of a background of

https://doi.org/10.1017/S0033583513000073 Published online by Cambridge University Press

fluorophores freely diffusing in solution and the controlled triggering of the biochemical reaction (Brewer & Bianco, 2008).

The most sophisticated approach in this category involves tethering a single DNA molecule between two optically trapped microspheres using dual-trap optical tweezers. In this way, it is possible to control both the tension and the extension of a single DNA molecule in a precise and dynamic fashion. These features are essential for high-resolution and high-sensitivity fluorescence imaging. It has been demonstrated that this approach allows manipulation of a DNA molecule with sub-piconewton resolution while visualizing individual fluorescent molecules bound to it. Hence, allowing determination of the oligomeric state as well as their physical location with sub-10-nm accuracy (Fig. 2) (Candelli *et al.* 2011; Comstock *et al.* 2011; Van Mameren *et al.* 2009a).

3. Single-molecule experiments

3.1 Assembly of the NPF

In the presynaptic phase of HR, the formation of the NPF is the first step catalysed by RecA and RAD51 recombinases (San Filippo *et al.* 2008). A two-step mechanism involving nucleation and growth has been proposed for the formation of a recombinase filament (Chabbert *et al.* 1987), but a precise quantification of both nucleation and growth rate has not been possible using standard bulk biochemical assays. Furthermore, full understanding of the mechanism of nucleoprotein-filament formation requires detailed knowledge of the oligomeric state of the recombinases in solution their multimerization kinetics and the DNA-binding properties of the different oligomeric states (Takahashi, 1989). In the following section, we will examine and discuss the major findings on the dynamic assembly of the NPF provided by single-molecule technologies. The assembly of both RecA and RAD51 recombinase filaments on ss and dsDNA was addressed using a diverse set of single-molecule techniques, including magnetic and optical tweezers, FRET spectroscopy and single-molecule fluorescence microscopy.

Using magnetic tweezers, changes in end-to-end length of DNA covered with RecA or RAD51 NPF were measured in real time (Figs 3 and 4) (Van der Heijden *et al.* 2007; Van Loenhout *et al.* 2009). Monte-Carlo simulations were performed to extract kinetic parameters characterizing RAD51 and RecA assembly (Van der Heijden & Dekker, 2008). On basis of these simulations, the authors proposed that RAD51-filament formation is characterized by: (i) a low ratio between growth and nucleation rate (cooperativity), approximately 200 for RAD51; (ii) pentamers of RAD51, preassembled in solution, being the units of filament nucleation and growth; (iii) RAD51-filament assembly being independent of the DNA being double- or single stranded and the tension applied to the DNA. The same experimental method and analysis were also applied to *E. coli* RecA, and its filament formation mechanism on ssDNA was addressed (Van Loenhout *et al.* 2009). Similarly to RAD51, the data suggested that RecA assembly on ssDNA occurs by nucleation and growth of preformed multimers of RecA (hexamers) that form filaments with low cooperativity (between 10 and 20).

In another, technically innovative magnetic-tweezers study (Arata *et al.* 2009), RAD51 binding to dsDNA was monitored by tracking changes in dsDNA twist instead of length. According to structural studies, the binding of RAD51 results in the elongation and unwinding of duplex DNA: each RAD51 monomer binding to dsDNA increases dsDNA length with 0.17 nm and unwinds it of approximately 45° (Yu *et al.* 2001). To monitor the rotation of the magnetic bead

https://doi.org/10.1017/S0033583513000073 Published online by Cambridge University Press

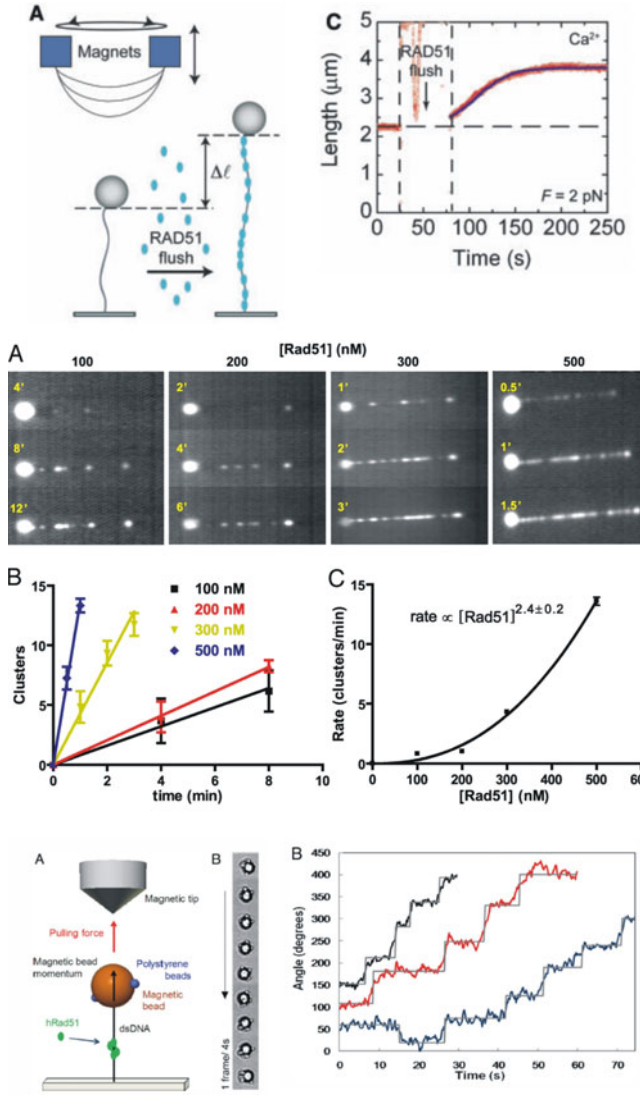


Fig. 3. RAD51 NPF formation at the single-molecule level. (*A*) Magnetic tweezers assay for studying the assembly of a recombinase protein on ssDNA and dsDNA. Constant tension is applied across a DNA molecule using a paramagnetic bead and a pair of permanent magnets. Binding of RAD51 induces a change in the end-to-end distance, which can be monitored in real time. (*B*) DNA length is monitored as a function of time before and after flushing RAD51 in the flow-cell. The increase in DNA length follows a typical profile that can be further analysed in order to estimate the parameters of RAD51 filament formation including nucleation and growth rate. (*C*) Free rotation magnetic tweezers technique. The magnet configuration produces a magnetic field in the z-direction, allowing the bead to freely rotate. (*D*) Sequence of video images showing the bead rotational movement produced by the loading of RAD51 on dsDNA. (*E*) Rotation traces at different RAD51 concentration show a stepping behaviour with a typical step size of 65° (black-10 nM, red-75 nM, blue-50 nM). (*F*) Single optical trapping combined with flow stretching and microfluidics is used to visualize the nucleation of RAD51 on dsDNA. Fluorescent snapshots are taken at different time points using increasing concentrations of RAD51 (from 100 to 500 nM) reveal the formation of multiple nuclei. (*G*) The clusters formation can be quantified as a function of time, showing a linear dependence on the time. (*H*) Nucleation rate can be plotted as a function of free RAD51 concentration, showing a non-linear dependence. The experimental data can be fitted with a using a power law with a 2.4 exponent. Figures reprinted from (Arata *et al.* 2009; Hilario *et al.* 2009; Van der Heijden *et al.* 2007).

https://doi.org/10.1017/S0033583513000073 Published online by Cambridge University Press

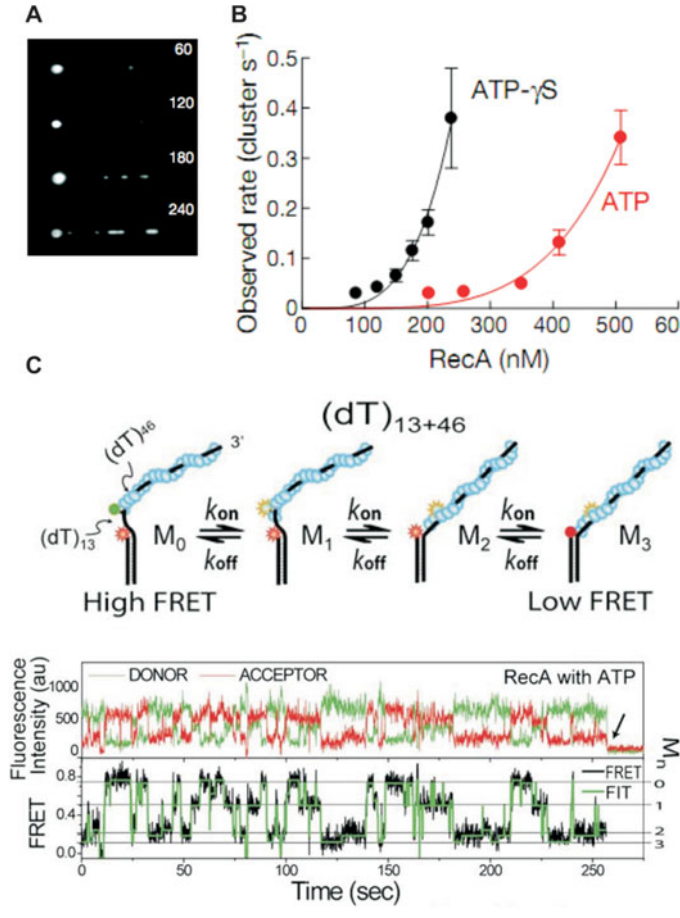


Fig. 4. RecA assembly studied using fluorescence visualization and FRET spectroscopy. (*A*) Optical tweezes combined with flow stretching for studying RecA assembly on dsDNA. Snapshots taken at different incubation times show a drastic increase in the fluorescence intensity along the DNA molecule, corresponding to RecA binding to dsDNA. (*B*) Quantification of RecA nucleation rate (appearance of fluorescent cluster along the DNA molecule) at different RecA concentrations in the presence of ATP (red dots) and ATP-γ-S (black). Fit corresponds to the functions $k_{\mathrm{nucl}} = k[\mathrm{RecA}]^n$. The value found for the parameter n was very similar for both nucleotide cofactors used in the experiment and was 4.5 ± 0.5 for ATP and 4.0 ± 0.4 ATP-γ-S. (*C*) Schematic representation of FRET-based assay for determining the extension unit of RecA filament assembly. A donor–acceptor FRET pair was positioned 13 nucleotides apart and RecA dynamics at the 5′-end of the filament could be observed by monitoring the FRET fluctuations in real time. (*D*) Four distinct FRET states were observed. Interestingly fast and reversible transitions occurred between states, indicating that association and dissociation of RecA was taking place. The transitions between FRET states were predominantly occurring between neighbouring states ($M_i \rightleftharpoons M_{i+1}$), indicating that the fundamental unit regulating assembly and disassembly is a RecA monomer. Figures reprinted from (Galletto *et al.* 2006; Joo *et al.* 2006).

along the vertical axis in response to RAD51 binding, a magnetic field parallel with the DNA was applied (Fig. 3). A smaller microsphere was attached to the paramagnetic bead connected to the DNA, allowing tracking of bead rotation with an accuracy of 5° (Fig. 3). Using this method, individual rotation steps of 65° were observed (Fig. 3), inconsistent with preassembled RAD51 pentamers being the active species for filament growth (Van der Heijden *et al.* 2007). On basis

https://doi.org/10.1017/S0033583513000073 Published online by Cambridge University Press

of these observations, the authors proposed a new model, where individual RAD51 monomers are responsible of the filament growth step. A single-molecule approach able to directly visualize the nucleoprotein-filament assembly made use of optical tweezers in combination with DNA flow-stretching and fluorescence microscopy (Galletto *et al.* 2006). A DNA molecule attached to a micron-sized bead held in an optical trap was extended using buffer flow. The instrument consisted of a micro-fluidic device that allow introduction of each reaction component separately using laminar flow. In this way, it was possible to expose the DNA molecule to a buffer containing fluorescently labelled RecA for a defined duration. Following this incubation step, the molecule was repositioned in an observation channel, which did not contain fluorescent RecA. Using this experimental assay, it was for the first time possible to directly visualize individual RecA nuclei on dsDNA and to quantify the rate of nucleation (of the order of 10^{-6} nuclei s^{-1} bp^{-1}) (Fig. 4) It was observed that the rate of nucleation, the rate-limiting step of filament formation, depends on RecA concentration with a power law (Fig. 4). Fitting the experimental data with the equation $k_{nucl} = k[\mathrm{RecA}]^n$ indicated that the nucleation step involves approximately 4–5 RecA monomers ($n = 4.5 \pm 0.5$). In addition, the RecA-filament nucleation phase could be distinguished from the growth phase by performing multiple, subsequent incubation and visualization cycles. Growth occurred with a rate of ~ 2 RecA monomers per second, indicating that RecA–dsDNA filament formation is characterized by a high cooperativity, of the order of 10^6, which is higher than has been reported from the bulk biochemical assays (Takahashi, 1989). This difference might arise from the ability to discriminate better the nucleation and growth in single-molecule measurements.

The same experimental protocol was applied to study the assembly mechanism of human RAD51 (Hilario *et al.* 2009). Intriguingly, important differences were reported. First, for RAD51 nucleation was shown to involve 2–3 RAD51 monomers. Second, RecA requires only a few nucleation points that grow cooperatively to produce μm-long segments of continuously coated DNA molecule. RAD51, because of its lower cooperativity, reaches complete coverage of the DNA starting from many more nuclei that show limited growth. This observation is a clear indication that the cooperativity of RAD51–dsDNA filament formation is one or two orders of magnitude smaller that of RecA.

The RecA-filament-formation mechanism was addressed at high temporal resolution using spFRET (Joo *et al.* 2006), with a donor and acceptor fluorophore attached to ssDNA in order to measure ssDNA conformational changes upon filament formation. Without RecA bound, the ssDNA is in a coiled configuration, with donor and acceptor close, resulting in a high FRET efficiency (Fig. 4). RecA binding to ssDNA leads to the formation of a stiff and elongated NPF, resulting in an increased distance between donor and acceptor and consequently a lower FRET efficiency. Attaching the fluorophores to different locations on the DNA, permitted to compare the kinetics of filament formation on the 3′- and the 5′-end of the ssDNA. The authors observed in the first place that stable filament formation only took place only on substrates with a single-stranded overhang exceeding 17 nucleotides. Substrates with shorter ssDNA segments allowed only the transient formation of DNA–protein complexes. The hypothesis connected to this observation was that nucleation clusters composed of smaller structures than RecA pentamers are not stable enough to form a seed for filament formation. Next, RecA binding and unbinding rates were determined for both the 3′- and 5′-ends. These measurements indicated two interesting aspects of RecA-ssDNA interaction: (i) the unbinding rate is equal at the two ends and (ii) RecA filament formation is faster at the 3′-end. The differential assembly speed of RecA at opposite ends, rather than in differences in the disassembly kinetics is therefore the reason

https://doi.org/10.1017/S0033583513000073 Published online by Cambridge University Press

of polar growth displayed by RAD51. Finally, the detailed analysis of the FRET traces revealed that filament extension occurs via the addition of RecA monomers.

Very recently, a substantial advancement towards the understanding of RecA filament assembly has been made. Using a novel assay, Bell *et al.* (Bell *et al.* 2012) monitored RecA nucleation and growth on single-stranded binding protein (SSB)-coated ssDNA. First, a biotinylated dsDNA molecule was attached to a streptavidin-coated glass coverslip, it was subsequently denatured using an alkaline solution and then saturated with fluorescent SSB. Fluorescent RecA was introduced in the flow-cell and after a rinsing step fluorescence visualization was used to inspect the formation of a RecA–ssDNA complex. Successive cycles of incubation, buffer exchange and fluorescence visualization highlighted the complex mechanism of RecA filament formation on SSB-coated ssDNA. A first striking observation was that RecA nucleation increased quadratically with respect to RecA concentration. This suggested that RecA nucleation on SSB-coated ssDNA requires a critical nucleus composed of a dimer, rather than of a pentamer, as reported by the same group in an earlier study on dsDNA (Galletto *et al.* 2006). Also, the effects of recombinase mediators such as RecO, RecF and RecR (RecFOR complex) were tested at the single-molecule level using a dual-optical tweezers assay combined with fluorescence microscopy(Galletto *et al.* 2006). The analysis of these interactions highlighted the interplay between SSB dynamics on ssDNA, RecA nucleation and filament assembly. The authors proposed that RecA is in fact unable to form filaments on SSB-coated ssDNA and its assembly relies uniquely on the transient local unwrapping of SSB tetramers from the ssDNA. The role of RecOR and RecFOR complex is therefore to destabilize the ssDNA–SSB complex, giving the opportunity to RecA to form the NPF and allow the sequential steps of HR to take place.

As described, several controversies have emerged from the various single-molecule studies of recombinase filament formation and a definitive molecular model describing the kinetics of filament formation is still lacking.

Currently, several experiments have provided evidence supporting a nucleation step of RAD51 and RecA that requires three or more proteins bound to ssDNA and dsDNA. A consensus over the actual number has not been reached yet, and in addition, a physical and structural explanation for this minimal size requirement is missing. Whether RAD51 and RecA accomplish nucleation starting from preassembled species in solution or through the coincident binding of multiple monomers also remain controversial. In fact, neither RecA nor RAD51 are present in solution in a well-defined oligomeric state. The kinetics of recombinase multimerization in solution has been addressed using different approaches (Nomme *et al.* 2008; Takahashi, 1989). It was found that the oligomeric state of RAD51 and RecA is highly sensitive to buffer conditions and protein concentration, which are not always well known.

In addition, using single-molecule approaches such as magnetic and optical tweezers, it is possible to disentangle the filament growth phase from the nucleation step only if the two kinetic rates are highly separated (high cooperativity) (Pierobon *et al.* 2010). In magnetic tweezers experiment, for example, the binding of protein to the DNA is monitored by measuring changes in DNA length (or twist), averaging over multiple, simultaneously growing filaments. Techniques employing fluorescence visualization allow discriminating the dynamics of distinct filaments. Fluorescence methods, however, suffer from the high background signal of fluorescently labelled proteins in solution, which makes it very hard to visualize the progress of filament formation in real time. To overcome this problem, DNA molecules are subjected to cycles of incubation (in a buffer containing fluorescently labelled recombinase) and visualization (in a buffer

https://doi.org/10.1017/S0033583513000073 Published online by Cambridge University Press

not containing fluorescent proteins), resulting in only snapshots. In the near future, we believe that improved visualization methods, capable of limiting background-fluorescence, will allow visualization in real time the formation of RAD51 and RecA recombinase filament with single-monomer resolution and finally properly address these unresolved questions.

3.2 Conformational transitions of the NPF

The interplay between structural and functional properties of recombinase filaments has been intensely studied, in particular by electron microscopy. The general idea that has emerged is that both RecA and RAD51 filaments can adopt two conformations, an extended, active one with a pitch of ∼9–10 nm and a more compressed one, that is, at least 20% shorter (DiCapua *et al.* 1990; Yu *et al.* 2001). The structural heterogeneity present in recombinase filaments is commonly attributed to a conformational transition induced by ATP hydrolysis, which involves the rotation of the C-terminal subunit in RecA or N-terminal one in RAD51 (Yu *et al.* 2001). Interestingly, the two filament conformations have been argued to have different biochemical functions: the extended one is active in performing stand exchange, while the compressed one appears inactive and might represent an intermediate before filament disassembly (Bugreev & Mazin, 2004). Since electron microscopy can only provide static snapshots of these conformational changes, single-molecule techniques have been applied to address these dynamics transitions in real time. The mechanical properties of recombinase–DNA complexes were explored for the first time using optical tweezers in a set of pioneering experiments at the end of the 1990s in the laboratory of Bustamante. A remarkable behaviour was observed for RecA–ssDNA filaments assembled in the presence of ADP (Hegner *et al.* 1999). Upon successive stretching and relaxing of these filaments, the force–extension curves measured in the optical tweezers displayed notable hysteresis (Fig. 5). Extending the molecule to its contour length required forces up to 15 pN. Reaching this force-threshold resulted in a plateau-like lengthening, followed by a further force increase. The relaxation curve showed a substantial lengthening but a more regular behaviour (Fig. 5). Two alternative interpretations were put forward: (i) stretching the ssDNA induces a transition of the NPF from the compressed to the extended state or, (ii) free-RecA in solution can associate with gaps opening along the filament in a force-dependent and reversible way. The latter explanation could not be excluded since the experiments were performed in the presence of protein in solution. Later, similar results were obtained in a study using magnetic tweezers (Van Loenhout *et al.* 2009). RecA NPFs were assembled on ssDNA in the presence of ATP and Mg^{2+}, while the DNA's end-to-end length was monitored at a constant stretching force of 3 pN. Using micro-fluidics, buffers containing or lacking ATP could be flushed in reversibly, resulting in elongation or contraction of the DNA by at least 20% (Fig. 5). These experiments were conducted without RecA in solution, confirming that nucleotide exchange modulates the conformation of the RecA filaments.

Single recombinase filaments on dsDNA also appear to have different conformations, as has been demonstrated in flow-stretch experiments combined with fluorescence microscopy (Robertson *et al.* 2009). In these experiments, a fluorescently labelled dsDNA molecule was anchored to a glass surface and RAD51 was flowed into the micro-fluidics chamber. NPF formation was monitored by visualizing the change in length of the dsDNA (Fig. 5). Upon filament formation, the dsDNA length increased, corresponding with the formation of RAD51 filaments in the extended conformation. Removing RAD51 from solution induced a dramatic shortening of the DNA, until a final length was reached corresponding to a compressed

https://doi.org/10.1017/S0033583513000073 Published online by Cambridge University Press

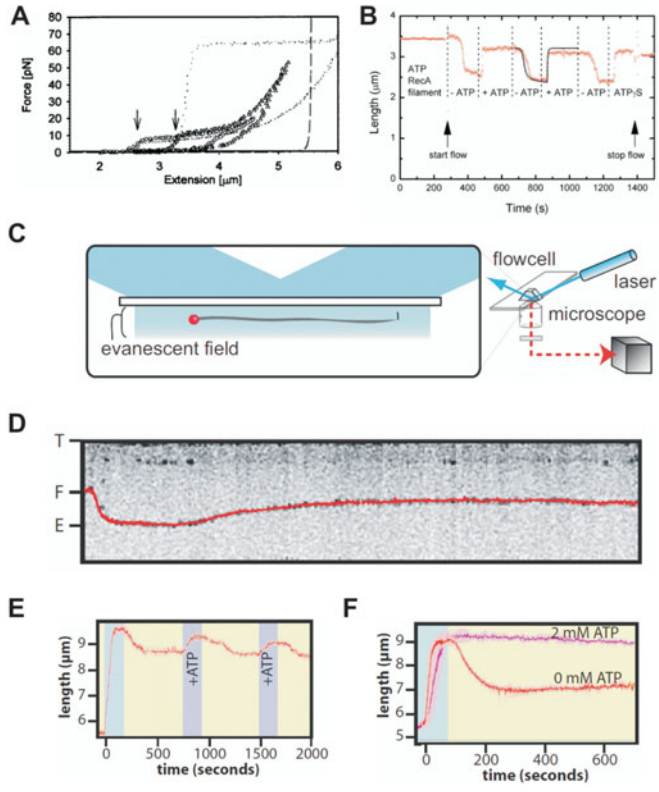


Fig. 5. Conformational transitions within RAD51 and RecA NPFs on dsDNA. (*A*) Consecutive stretching and releasing cycles of a single ssDNA molecule in complex with RecA–ADP using optical tweezers. The first stretching curve shows the approaching of the contour length approximately at the extension of 3 μm. At 10 pN a plateau is observed, followed by the sudden stiffening of the molecule. The release curve shows hysteresis, indicating the occurrence of a force-induced conformational transition. During the second force-extension cycle the contour length is reached at the extension of 2.5 μm but the elastic behaviour is qualitatively similar to the first extension-release cycle. (*B*) A RecA NPF is formed on ssDNA held at the force of 3 pN using magnetic tweezers in the presence of ATP. Multiple buffer exchanges containing or lacking ATP induce reversible changes in DNA-lengths. (*C*) TIRF-microscopy is combined with DNA flow-stretching for studying conformational changes within NPFs. (*D*) Example of experimental result showing the lengthening and successive shortening arising from NPF assembly and subsequent compression. (*E*) Cycles of buffer exchange show reversible transition of the NPF from the extended to compressed state and vice-versa resulting from the presence of free ATP in solution. (*F*) If after RAD51 assembly, ATP is depleted from solution (red trace) the nucleoprotein converts into its compressed form (final length $\sim$7 μm). When high ATP concentration is supplied to the reaction, the filament compression step is blocked. Figures reprinted from (Hegner *et al.* 1999; Robertson *et al.* 2009; Van Loenhout *et al.* 2009).

conformation. These results indicated that RAD51 could remain DNA-bound in the compressed form for a significant amount of time. At high ATP concentrations (2 mM), filament compression as well as disassembly were inhibited (Fig. 5). In addition, applying cycles of rapid buffer exchange between ATP-containing and ATP-free solutions resulted in reversible transitions between compressed and elongated filaments, without RAD51 detaching from the DNA (Fig. 5). This study clearly indicates that RAD51 filaments can also adopt distinct conformations, tightly coupled to the nature of the nucleotide bound.

https://doi.org/10.1017/S0033583513000073 Published online by Cambridge University Press

More recently, magnetic tweezers have been used to study whether force can induce conformational transitions in RecA–dsDNA filaments (Conover *et al.* 2011). In this study, single dsDNA molecules were first coated by RecA and then subjected to step-wise force increases and decreases, while monitoring their extension using video microscopy. In the absence of free RecA in solution, rapid (<1 s) force increases (from 40 to 55 pN) were followed by slow (4 nm s^{-1}) and continuous elongation of the DNA, lasting more than 100 s. This observation indicated that applying force to the filament can induce a conformational transition from the compressed to the elongated conformation, resulting in longer DNA tethers.

Single-molecule approaches have thus provided hints of the dynamic nature of recombinase filaments. Several studies have confirmed that both RecA and RAD51 form filaments on DNA differing in length and mechanical properties that can reversibly interchange. On the one hand, filaments in the compressed conformation (which appears to be inactive in catalysing strand exchange) can be converted to the extended configuration if a high-enough ATP concentration is present in solution. On the other hand, tension on the filament also affects filament conformation, indicating the tight coupling between the DNA substrate and the filament structure. Several of the molecular mechanisms underlying the transition between the extended, ATP-bound filament to the compressed, ADP-bound one are unclear. First of all, what is the temporal coordination between ATP hydrolysis, ADP release and the structural compression step? In addition, what structures are adopted when both ATP and ADP are present within the same filament? Is it possible that heterogeneous structures are present within the same continuous NPF? Furthermore, the quantitative thermodynamic model underlying the transition between these two conformations is not known. Future single-molecule experiments, in conjunction with non-equilibrium thermodynamic modelling will be required to gain further insights in this intriguing aspect of recombinase NPFs and their role in the strand exchange reaction.

3.3 Searching for a needle in the haystack

During the homology search process the recombinase NPF needs to find, align and form a stable complex with the complementary sequence on a duplex template. This process needs to be relatively fast and efficient, considering that replication takes approximately 1–2 h (in *Saccharomyces cerevisiae* (Aylon *et al.* 2003)) and in that time a unique sequence has to be found among the many millions of base pairs available. The strategy and mechanism of homology search is not clear at present. A mechanism purely involving one-dimensional (1D) sliding has been ruled out both experimentally (Adzuma, 1998) and from theoretical considerations (Barzel & Kupiec, 2008). Recently, the first direct insights in the homology search mechanism have been obtained using fluorescence microscopy in combination with dual-trap optical tweezers and microfluidics (Forget & Kowalczykowski, 2012). In this study, a single dsDNA molecule was manipulated using optical tweezers in order to control its end-to-end length. Using micro-fluidics and an automatized microscope stage (Fig. 6), the trapped DNA molecule was transferred into a reservoir with no buffer flow present, where it was allowed to interact with fluorescently labelled ssDNA molecules pre-incubated with RecA–ATP-γ-S . After a defined incubation time, the DNA was inspected using fluorescence microscopy. Stable strand-exchange complexes were observed by monitoring the binding of fluorescent NPFs to the homologous sequence in the optically trapped DNA (Fig. 6). It was found that the efficiency and speed of homology pairing decreased drastically when the dsDNA was held in an extended conformation. Stretching the target dsDNA (end-to-end length more than 80% of the contour length) resulted in no binding

https://doi.org/10.1017/S0033583513000073 Published online by Cambridge University Press

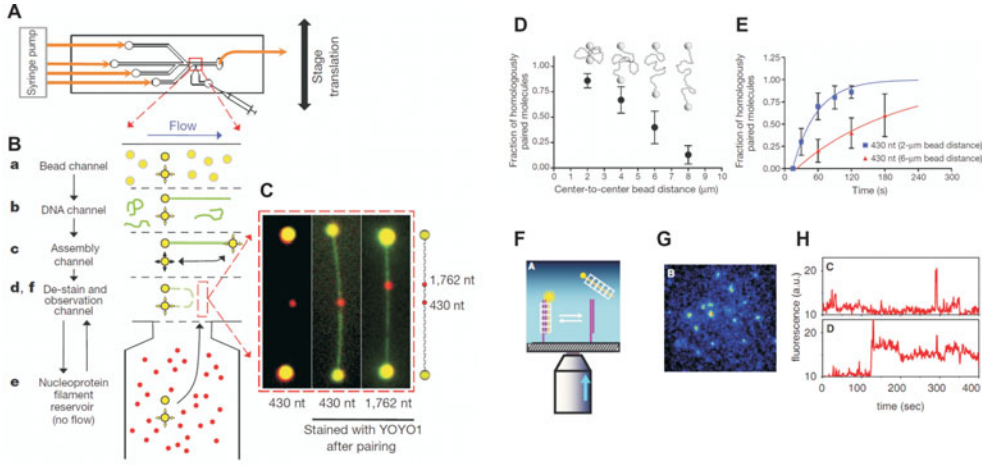


Fig. 6. Homology search mechanism performed by RecA NPFs. (*A*) Schematic representation of the five-channel microfluidic device used in the experiment. (*B*) Sequential multi-step assembly of the single-molecule assay. (a) Capturing two beads in the optical trap. (b) DNA tethering. (c) DNA manipulation and visualization. (d) YOYO destaining and set of end-to-end distance. (e) Incubation of the dsDNA with the reservoir containing the fluorescently labelled NPF. (f) Return in the imaging buffer and visualization of the formation of the strand exchange complex in the absence of fluorescence background. (*C*) Visualization of the end-product of the strand-exchange reaction. Two different fluorescent NPFs were used, of 430 and 1762 nucleotides respectively. Each of them is homologous to a different section of the Lambda DNA molecule used as a template. Fluorescence visualization allows confirming that strand-exchange took place at the correct position. (*D*) The efficiency of the strand-exchange complex formation shows a strong dependence on the conformation of the DNA molecule. At the distance of only 8 μm, corresponding to approximately 50% of the contour length of the DNA molecule the strand exchange reaction is highly efficient. (*E*) The speed of homologous recognition is strongly dependent on the DNA conformation. (*F*) TIRF-based assay for studying the synapsis lifetime. (*G*) Fluorescent image of synaptic complexes. (*H*) Fluorescence *versus* time for synapsis events using heterologous (top) or homologous (bottom) sequences. Figures reprinted from (Bell *et al.* 2012; Mani *et al.* 2010).

of homologous NPFs. On the other hand, when the target DNA molecule was relaxed (end-to-end length 20% of the contour length), strand-exchange complexes formed instantaneously. In addition, homology pairing was found to strongly dependent on the length of the NPF used in the experiment (Fig. 6). This finding appears to be inconsistent with a search mechanism solely relying on 1D sliding of the NPF along the target DNA. Additional modes of search need to be available, such as hopping (Gorman & Greene, 2008) and inter-segmental transfer (dissociation and re-association at a distal segments on the DNA) to explain the dependence of search kinetics on tension on the DNA and length of the NPF. The authors proposed a mechanism in which a long RecA NPF is simultaneously in contact with many segments of the target DNA (parallel homology sampling) through short, reversible synapsis events. When the DNA is not stretched, all conformations can be explored due to Brownian motion, allowing the NPF to interact with distant DNA segments within short time intervals and therefore accelerating the search process.

Another set of single-molecule fluorescence experiments addressed the issue of discriminating between homologous and non-homologous sequences in the search process by quantifying how the lifetime of the synaptic complex depends on the degree of homology (Mani *et al.* 2010). In the assay used, short dsDNA molecules were anchored to a glass surface while fluorescently labelled RecA-coated ssDNA molecules were introduced. Stable complex formation between target

https://doi.org/10.1017/S0033583513000073 Published online by Cambridge University Press

DNA and NPFs were identified by stable and bright fluorescence spots appearing on the glass surface (Fig. 6). It was found that completely heterologous sequences did form complexes with lifetimes of tens of seconds. Fully homologous sequences, on the other hand were found to be even more stable, with lifetimes of hundreds of seconds. In addition, single mismatches were shown to significantly decrease the synapsis stability.

An innovative study, employing the simultaneous manipulation of two DNA molecules, aimed at quantifying the thermodynamics aspects of synaptic complex (Fig. 7) (De Vlaminck *et al*. 2012). In that assay, a dsDNA molecule was tethered between two optical traps and subsequently melted by applying a high tension resulting in a tethered ssDNA molecule (Gross *et al*. 2011; Van Mameren *et al*. 2009b). This ssDNA molecule was incubated with RecA in the presence of ATP-γ-S to obtain a stable RecA–ssDNA filament. In addition to optical tweezers, the experimental setup also consisted of magnetic tweezers, used to independently stretch and twist a dsDNA molecule tethered to a glass surface. The ssDNA–RecA complex was brought in contact with the dsDNA and interactions between both DNA molecules were assessed. The first experimental goal was to quantify the interaction between the secondary binding site of the RecA filament and the target dsDNA. Positively twisted and uncoiled dsDNA did not interact with the NPF, while slightly stretched (tension 3.5 pN) and negatively supercoiled dsDNA did interact (Fig. 7). Increasing negative supercoiling resulted in increased strength and probability of interacting with the NPF. It was proposed that the negative supercoiling makes short segments of ssDNA available by the transient formation of ssDNA bubbles on the target dsDNA. These ssDNA segments, due to their high affinity for the secondary binding site of RecA filaments (Mazin & Kowalczykowski, 1996) stabilize the strand-exchange complex. The need for negative supercoiling for observing interactions indicates that the secondary binding site alone is not able to provide the necessary energy for melting the target dsDNA and forming a complex with the ssDNA. Spontaneous DNA breathing and supercoiling, therefore, appear to play important roles in the homology search process. In order to be tested for homology, the target dsDNA needs to be first opened and distorted substantially from its native B-form structure, resulting in an energy penalty. When homology is found the energy penalty can be overcome by the base-pairing energy that is gained (Fig. 7). This model therefore provides a quantitative framework for the detailed energetic balance leading to successful sequence recognition.

In conclusion, the energetics and kinetics of the reaction intermediates leading to the formation of a stable synapse have been addressed at the single-molecule level. Several aspects of this process, however, are still unclear. In the first place, a quantitative model explaining how DNA conformational dynamic affects the efficiency and the speed of the homology search process is still missing. Secondly, the observation that heterologous DNA molecules can pair with high stability in presence of RecA is in apparent contradiction with the requirement of the homology search process to scan fast through the large amount of non-complementary sequences. In addition the experimental assays employed so far were not yet able to directly visualize the actual process of search and recognition of homology and were rather indirect in detecting the intermediate steps leading to a stable D-loop formation. Furthermore, the relative balance between 1D and 3D diffusive mechanisms during homology search is still not known. Although the first experiments addressing the thermodynamic aspects underlying the formation of a stable DNA–nucleoprotein complex have been performed, a precise quantification of the lifetime of the intermediates states is required to elaborate a predictive target–search model explaining how two complementary sequences find each other in the genomic haystack.

https://doi.org/10.1017/S0033583513000073 Published online by Cambridge University Press

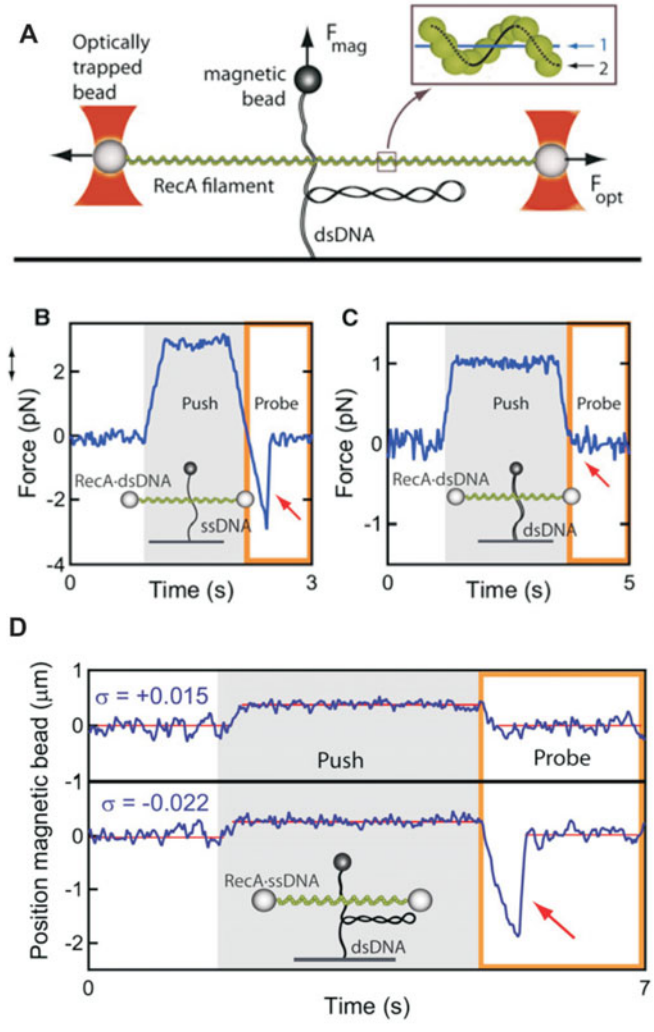


Fig. 7. Dual-DNA manipulation to study RecA-mediated strand exchange. (*A*) Dual-optical trap is used to manipulate a RecA–DNA (either ssDNA or dsDNA) complex. Magnetic tweezers is used to stretch and twist a second DNA molecule (either ssDNA or dsDNA) tethered between the glass surface and a magnetic bead. The two DNA molecules can be brought into contact and slided next to each other to probe their interaction. (*B*) Push-probe experiment between a RecA–dsDNA complex and an ssDNA. A force of ∼3 pN is required to disrupt the complex. (*C*) Push-probe experiment between a RecA–dsDNA and dsDNA. No interaction is observed. (*D*) Effect of positive and negative supercoils of dsDNA molecule. When positive supercoils are applied no interaction is observed (top panel). When negative supercoils are instead applied, a stable complex is formed that requires a force of ∼2 pN to be disrupted. Figures reprinted from (De Vlaminck *et al.* 2012).

3.4 Strand-exchange at the single-molecule level

The NPF, after finding the homologous sequence, catalyses the defining event of the HR process: the transfer of information between homologous sequences, the strand-exchange. Owing to its transient nature, it has been very difficult to isolate and study this key-step of HR using bulk biochemical or structural methods. Single-molecule approaches have tackled this

https://doi.org/10.1017/S0033583513000073 Published online by Cambridge University Press

problem, addressing its molecular mechanism in real time on single DNA molecules. In the first single-molecule study of strand exchange, a dsDNA molecule was attached to a glass surface stretched and negatively supercoiled ($F = 0.5$ pN and 35 negative rotations). The changes in twist and end-to-end length of the tethered DNA molecule were monitored, while it was strand-invaded by homologous RecA–ssDNA filaments of different lengths (Fig. 8) (Van der Heijden *et al.* 2008). As DNA bound by RecA is elongated and unwound, strand-exchange results in the removal of negative supercoils, which in turn corresponds to a drastic elongation of the torsionally constrained DNA. The experiment was performed preassembling RecA on ssDNA using two different nucleotide cofactors: ATP-γ-S and ATP. When ATP-γ-S was present, a gradual and steady increase in the tether length was observed. The final length was compatible with the expected unwinding and stretching due to the invasion of the homologous DNA segment. In fact, both the final elongation as well as the duration of the length increase was linearly dependent on the size of the invading filaments. Therefore, it was possible to provide an estimate of the strand-exchange rate, which was found to be approximately $2\ \mathrm{bp\ s^{-1}}$. Substituting ATP-γ-S with ATP resulted in a drastically different behaviour. In this case, after an initial phase in which the DNA length started to increase, a long plateau was observed, followed finally by a decrease in length until the original DNA extension was reached. Two analysis methods were applied: in the first one, the total interaction time was quantified (length increase + plateau + length decrease). This quantity was also found to be proportional to the size of the invading recombinase filament, following the same linear dependence found for the ATP-γ-S. In the second analysis method, the duration and amount of the length increase phase were quantified. It was observed that they show no correlation with the length of the invading RecA filament. A hypothesis was formulated, in which under ATP-hydrolysis conditions, strand exchange progresses throughout the homologous region only through a region (strand-exchange window) composed of 80 bases. In this model, the exchange starts at one the invading end (5′), with a rate that is equal to ATP-triggered RecA unbinding. The invading filament locally elongates and unwinds the tethered molecule, increasing the end-to-end distance. At the lagging end, instead, RecA release into solution after ATP hydrolysis and a new heteroduplex is created. Therefore, while strand exchange progresses in ATP-hydrolysing conditions, the end-to-end distance remains constant (Fig. 8). After the reaction is completed, and all RecA proteins dissociated, a three-stranded joint structure is obtained, whose length is identical to the initial length.

In a second study, spFRET was used to study RecA-catalysed strand-exchange, allowing discrimination between docking of a RecA–ssDNA complex to the target dsDNA and further progression of strand exchange (Ragunathan *et al.* 2011). The experimental configuration used in the experiment is schematically represented in (Fig. 8). Acceptor-labelled RecA–ssDNA NPFs were assembled in the presence of ATP-γ-S and immobilized. Donor-labelled dsDNA was injected into the flow-cell and both donor and acceptor fluorescence intensities were monitored upon donor excitation. An example of an experimental result is shown in Fig. 8. After an initial lag phase, the donor fluorescence signal suddenly increased (due to the docking of the donor-labelled dsDNA). This state quickly converted (during an interaction time $\Delta t_{\mathrm{delay}}$) to a more stable configuration, characterized by a high FRET efficiency, interpreted to represent the final strand-invaded complex. The design of the DNA substrates revealed that the initial binding of the duplex DNA to the NPF (docking) occurred at different random positions involving just a few bases. The irreversible conversion from this intermediate state to a high FRET value was interpreted as the actual occurrence of the strand exchange reaction. Therefore, the distribution

https://doi.org/10.1017/S0033583513000073 Published online by Cambridge University Press

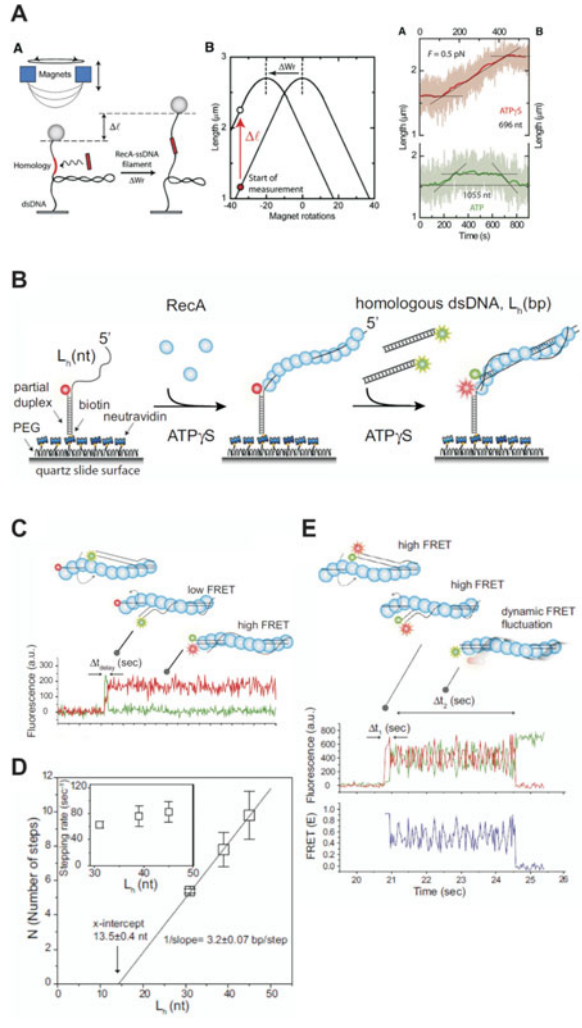


Fig. 8. Strand exchange dynamics at the single-molecule level. (*A*) A single dsDNA molecule is held at constant force and negatively supercoiled using magnetic tweezers. Strand-exchange results in the increase of the end-to-end length of tether and a shift in the rotational offset of the rotation–extension curve (see (*B*)). (*C*) Real-time detection of the strand exchange reaction in the absence (red curve) and presence of ATP hydrolysis (green curve). Absence of hydrolysis produces an irreversible lengthening of the DNA tether which is compatible with a three-stranded structure having a pitch of 14.6 bp/turn and an elongation of 0.51 nm bp^{-1}. When ATP hydrolysis is permitted the lengthening is only transient and corresponds to a moving strand exchange windows of 80 bases. (*B*) A partial duplex DNA molecule is attached to a quartz glass slide trough a biotin–neutravidin bond. A fluorescent molecule (donor) is covalently attached at the single–double-stranded DNA junction. A single-stranded tail with a 5′-end of various length is used to assemble the RecA NPF in the presence of ATP-γ-S. (*C*) A donor-labelled dsDNA FRET time trace showing a sudden increase in donor fluorescence (docking), followed by a gradual transition to a high FRET value ($\Delta t_{\mathrm{delay}}$). (*D*) The number of steps before the completion of the strand exchange reaction is plotted against the homology length. The strand exchange reaction occurs at the speed of 3.2 bp $step^{-1}$ and requires the initial docking of 13.5 nucleotides. (*E*) Strand separation assay using a donor–acceptor-labelled duplex DNA reveals fast FRET fluctuations, indicating that the outgoing strand interacts with the secondary binding site of the RecA–ssDNA filament. Figures reprinted from (Ragunathan *et al.* 2011; Van der Heijden *et al.* 2008).

https://doi.org/10.1017/S0033583513000073 Published online by Cambridge University Press

of strand-exchange times (Δt_{delay}, the delay time between the formation of the first intermediate and the stable highest FRET configuration) was fitted with a Gamma distribution ($\Delta t^{N-1}e^{-k\Delta t}$), under the assumption that strand exchange involves N-hidden rate-limiting steps. Performing this analysis with substrates of different lengths indicated that strand invasion proceeds in steps involving three bases and is characterized by a stepping rate of $\sim$70 bp s^{-1} (Fig. 8). The observation that strand invasion occurs in 3 bp steps is in good agreement with high-resolution structural data (Chen *et al.* 2008), which shows that bases in the RecA–ssDNA complex are grouped in triplets. A remarkable behaviour was observed when monitoring the dynamics of the displaced strand of the dsDNA, which is displaced by the NPF. After an initial docking phase (Δt_1), a phase lasting $\sim$3 s involving rapid fluctuations in FRET efficiency was detected (Fig. 8). The authors proposed that these fluctuations are the results of intermittent interactions between displaced DNA strand and the secondary binding site on the RecA filament.

How recombinase filaments mediate the transfer of strands from one DNA molecule to the other remains largely obscure. The two single-molecule experiments presented, which addressed this key biological step, present important differences and few similarities. First of all, the estimated strand-exchange rates are very different (70 bp s^{-1} in the spFRET experiment and 2 bp s^{-1} in the magnetic tweezers study). One possible explanation is that strand exchange is highly sensitive to the torsional constrains imposed on the target DNA molecule (the DNA ends are free in the spFRET experiment and engaged by the glass and bead surfaces in the magnetic tweezers experiment) and the buffer conditions used (100 mM sodium acetate and 10 mM magnesium acetate in the spFRET experiment and 10 mM $MgCl_2$ in the magnetic tweezers experiment). As strand-exchange can proceed in the absence of ATP hydrolysis, it is likely that experimental circumstances affecting the stability of the DNA duplex, such as electrostatic screening and supercoiling, play important roles in determining how fast the two strands exchange. Both studies, in fact, point to a model in which the breathing dynamics of the double helix could play a crucial role in determining the kinetics of the strand-exchange reaction, as anticipated by bulk studies (Bazemore *et al.* 1997; Gupta *et al.* 1999; Xiao *et al.* 2006). Finally, what is the driving force behind the directionality and progression of the strand exchange reaction? How can unidirectional motion be obtained in the absence of ATP hydrolysis between two states having an equal amount of paired DNA bases? Fortunately, due to the rapid development of single molecules techniques, it is expected that these questions will be addressed in the near future.

3.5 RAD51 disassembly from DNA

The final step of HR is the disassembly of recombinase proteins from dsDNA. Disassembly of RAD51 filaments has been examined by the previously described optical tweezers/flow-stretching strategies (Fig. 2) (Hilario *et al.* 2009). In one paper, the filament disassembly was monitored in different buffer conditions after forming the RAD51 filaments in the presence of ATP and either Ca^{2+} or Mg^{2+}, When RAD51 filaments were assembled in Ca^{2+}–ATP conditions and successively exposed to Mg^{2+} (in the presence of ATP) they did not disassemble (Fig. 9). It is well known that Ca^{2+} induces and preserves the active and extended conformation of the RAD51 filament, by blocking ATP hydrolysis (Bugreev & Mazin, 2004). To explain this observation the authors implicated the slow exchange of the divalent cation bound to RAD51. In contrast, RAD51 filaments formed and visualized in a buffer containing Mg^{2+}–ATP (in the absence of Ca^{2+}), allowing ATP hydrolysis, showed clear signs of filament

https://doi.org/10.1017/S0033583513000073 Published online by Cambridge University Press

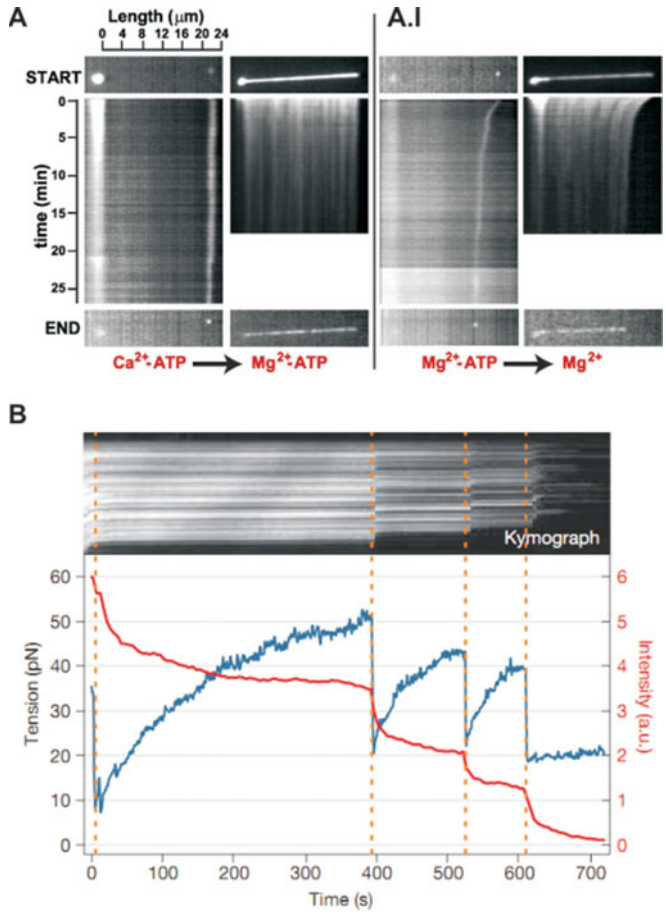


Fig. 9. RAD51 disassembly from dsDNA. (*A*) Flow-stretching assay for characterizing RAD51 disassembly. RAD51 filaments (RAD51 on the left and RAD51-fluorescein on the right) are assembled in the presence of $CaCl_2$ and disassembly is observed in the presence of $Mg(OAc)_2$. A very slow reduction in the DNA-length is observed. [A.I] DNA–RAD51 filaments assembled in the presence of $Mg(OAc)_2$ shows a significant reduction in length when exposed to a buffer lacking ATP. Disassembly, does not complete after a period of 25 min as can be seen from the presence of fluorescent RAD51 bound along the DNA molecule. (*B*) The effect of DNA tension on RAD51 disassembly studied using dual-optical trapping and fluorescence microscopy. RAD51–dsDNA filaments are formed in the presence of $CaCl_2$ and disassembly is observed in $MgCl_2$. The trap position is kept constant. Disassembly induces a fluorescence intensity drop (red line) and a correlated force increase (blue line). Disassembly eventually stalls when the force reaches forces of 50 pN ($t \sim 400$ s). Releasing the tension to 20 pN ($t \approx 400$ s) allows the disassembly reaction to reinitiate, generating tension across the DNA. The process can be repeated further until complete disassembly of RAD51 is achieved. Figures reprinted from (Hilario *et al.* 2009; Van Mameren *et al.* 2009a).

disassembly: shortening of the dsDNA and disappearance of the fluorescent RAD51. Remarkably, not all RAD51 disassembled from the DNA presumably because ADP-bound RAD51 filaments remained bound to dsDNA for surprisingly long times, in the order of tens of minutes. The existence of a long-lived RAD51-bound state subsequent to ATP hydrolysis has important consequences for the progression of the HR *in vivo*, blocking the following steps of the reaction. The authors proposed that recombinase modulators such as the translocating motor RAD54 are needed to fully disassemble ADP-bound NPFs.

https://doi.org/10.1017/S0033583513000073 Published online by Cambridge University Press

A different approach, involving dual-trap optical tweezers, quantitative single-molecule fluorescence microscopy and microfluidics provided more detailed insight in filament disassembly. In contrast to the flow-stretching approach discussed above, the use of two optical traps allows a well-defined tension to be applied on the tethered DNA, constant over its whole length (Van Mameren *et al.* 2009a) (Fig. 9). Using this approach, it was observed that high tensions slow down RAD51-disassembly, effectively stalling the process at forces above 50 pN, even under conditions favouring ATP hydrolysis. Upon a sudden release of the tension, large bursts of RAD51 disassembly were observed. Furthermore, RAD51 disassembly did not occur in a continuous manner, but in bursts, interrupted by pauses, with exponentially distributed duration. A new model for RAD51 disassembly was proposed in which (i) ATP hydrolysis occurs throughout the filament, independently of the applied tension (ii) RAD51 monomers within the filament (and not on one of the ends) remain DNA bound, irrespective of the nucleotide bound (ATP or ADP). (iii) RAD51 monomers at filament ends detach from the DNA after ATP hydrolysis. The actual detachment (and not ATP hydrolysis) depends on tension: at low tension monomers fall off almost instantaneous (until an ATP-bound RAD51 remains on the end), at high tension (50 pN), detachment can be totally counteracted. To explain the force-dependent dissociation rate, it was hypothesized that the complex between dsDNA and an RAD51 monomer on a filament end has to contract, before detachment can take place. This contraction is counteracted by applying tension on the DNA. The elastic energy stored in the filament due to the DNA elongation (dsDNA is lengthened by 50% compared with its B-form when in complex with RAD51 or RecA) is therefore the driving force for the release of the NPF from the dsDNA.

These results provide an alternative explanation for the incomplete filament disassembly in the flow-stretching experiments discussed above (Hilario *et al.* 2009). In that experiment, the DNA was extended using flow stretching with a solution containing a high sucrose concentration (10% w/v). This method is probably capable of exerting high-enough tensions to severely influence the disassembly process. Despite this inconsistency, both single-molecule studies propose possible molecular strategies to efficiently remove RAD51 from dsDNA. One option, for example would consists in increasing the rate of ATP hydrolysis only at the filament-end and exploiting the natural hydrolysis rate of RAD51 to catalyse the low-affinity DNA-binding state rather than actively wiping off RAD51 by RAD54 translocation through DNA-bound RAD51 filaments. A second open question concerns the molecular mechanism of RAD51 disassembly. Specifically, the temporal coordination between the ATP-hydrolysis, the structural change and the release into solution is unknown. Also, the structural reason why individual monomers cannot dissociates from internal regions of the filament but only from disassembling ends is unclear.

4. Conclusions and outlook

As discussed in detail above, over the last two decades, single-molecule approaches have tremendously aided deciphering the individual steps of genetic recombination. DNA manipulation and fluorescence visualization have resulted in a better understanding of recombinase-filament assembly dynamics: the rate-limiting step is nucleation on the DNA, involving two to six recombinase monomers. Force-extension measurements have identified dynamics between different conformations of recombinase filaments and how these dynamics depend on ATP-hydrolysis state. Homology search and strand exchange have been studied in separation, resulting in numerous insights in this enigmatic processes. Finally, DNA flow-stretching and optical

https://doi.org/10.1017/S0033583513000073 Published online by Cambridge University Press

tweezers studies in combination with fluorescence microscopy have enabled the study of recombinase disassembly at the level of individual recombinase monomers, shedding light on the interplay between disassembly, conformational change and nucleotide hydrolysis.

Future technological and theoretical developments will permit further elucidation of important questions in HR research. For example, the physical and structural basis of the number of recombinase monomers required for nucleation is still under intense debate. Also direct visualization and characterization of the reaction intermediates in homology search and strand exchange would help to obtain better insight in these processes. Another future challenge lies in studying the role of the many mediators involved in assisting recombinases to perform HR. Such measurements will serve in the verification of existing hypotheses on HR regulation and might shed new insights in the mechanisms of DNA repair.

5. Acknowledgements

This work was supported by Netherlands for Scientific Research (NWO). A. C. is recipient of a NWO TopTalent grant. E. J. G.P., G. J. L.W. and C. W. are recipients of a NWO VICI grant. G. J. L.W. is recipient of an ERC Starting grant. M. M. acknowledges support from the Agence Nationale pour la Recherche (grant no. ARN 2010 Blanc 1521 01 project RADORDER) and the Foundation ARC pour la Recherche sur le Cancer (grant no. A09/2/5075).

6. References

Abbondanzieri, E. A., Greenleaf, W. J., Shaevitz, J. W., Landick, R. & Block, S. M. (2005). Direct observation of base-pair stepping by RNA polymerase. *Nature* **438**, 460–465.

Adzuma, K. (1998). No sliding during homology search by RecA protein. *Journal of Biological Chemistry* **273**, 31565–31573.

Arata, H., Dupont, A., Miné-Hattab, J., Disseau, L., Renodon-Cornière, A., Takahashi, M., Viovy, J.-L. & Cappello, G. (2009). Direct observation of twisting steps during Rad51 polymerization on DNA. *Proceedings of the National Academy of Sciences of the United States of America* **106**, 19239–19244.

Ashkin, A., Dziedzic, J. M., Bjorkholm, J. E. & Chu, S. (1986). Observation of a single-beam gradient force optical trap for dielectric particles. *Optics Letters* **11**, 288.

Aylon, Y., Liefshitz, B., Bitan-Banin, G. & Kupiec, M. (2003). Molecular dissection of mitotic recombination in the yeast Saccharomyces cerevisiae. *Molecular and Cellular Biology* **23**, 1403–1417.

Barzel, A. & Kupiec, M. (2008). Finding a match: how do homologous sequences get together for recombination? *Nature Reviews Genetics* **9**, 27–37.

Baumann, P., Benson, F. E. & West, S. C. (1996). Human Rad51 protein promotes ATP-dependent homologous pairing and strand transfer reactions *in vitro*. *Cell* **87**, 757–766.

Bazemore, L. R., Folta-Stogniew, E., Takahashi, M. & Radding, C. M. (1997). RecA tests homology at both pairing and strand exchange. *Proceedings of the National Academy of Sciences of the United States of America* **94**, 11863–11868.

Bell, J. C., Plank, J. L., Dombrowski, C. C. & Kowalczykowski, S. C. (2012). Direct imaging of RecA nucleation and growth on single molecules of SSB-coated ssDNA. *Nature* **491**, 274–278.

Benson, F. E., Stasiak, A. & West, S. C. (1994). Purification and characterization of the human Rad51 protein, an analogue of E. coli RecA. *EMBO Journal* **13**, 5764–5771.

Blainey, P. C., van Oijen, A. M., Banerjee, A., Verdine, G. L. & Xie, X. S. (2006). A base-excision DNA-repair protein finds intrahelical lesion bases by fast sliding in contact with DNA. *Proceedings of the National Academy of Sciences of the United States of America* **103**, 5752–5757.

Brewer, L. & Bianco, P. (2008). Laminar flow cells for single-molecule studies of DNA-protein interactions. *Nature Methods* **5**, 517–525.

Bugreev, D. V. & Mazin, A. V. (2004). Ca2+ activates human homologous recombination protein Rad51 by modulating its ATPase activity. *Proceedings of the National Academy of Sciences of the United States of America* **101**, 9988–9993.

Candelli, A., Wuite, G. J. L. & Peterman, E. J. G. (2011). Combining optical trapping, fluorescence microscopy and micro-fluidics for single molecule studies of DNA-protein interactions. *Physical Chemistry Chemical Physics: PCCP* **13**, 7263–7272.

https://doi.org/10.1017/S0033583513000073 Published online by Cambridge University Press

Cerbinskaite, a., Mukhopadhyay, a., Plummer, E. R., Curtin, N. J. & Edmondson, R. J. (2012). Defective homologous recombination in human cancers. *Cancer Treatment Reviews* **38**, 89–100.

Chabbert, M., Cazenave, C. & Hélène, C. (1987). Kinetic studies of recA protein binding to a fluorescent single-stranded polynucleotide. *Biochemistry* **26**, 2218–2225.

Chen, Z., Yang, H. & Pavletich, N. P. (2008). Mechanism of homologous recombination from the RecA-ssDNA/dsDNA structures. *Nature* **453**, 489–484.

Comstock, M. J., Ha, T. & Chemla, Y. R. (2011). Ultrahigh-resolution optical trap with single-fluorophore sensitivity. *Nature Methods* **8**, 335–340.

Conover, A. J., Danilowicz, C., Gunaratne, R., Coljee, V. W., Kleckner, N., & Prentiss, M. (2011). Changes in the tension in dsDNA alter the conformation of RecA bound to dsDNA-RecA filaments. *Nucleic Acids Research* **39**, 8833–8843.

Conway, A. B., Lynch, T. W., Zhang, Y., Fortin, G. S., Fung, C. W., Symington, L. S., & Rice, P. A. (2004). Crystal structure of a Rad51 filament. *Nature Structural and Molecular Biology* **11**, 791–796.

Dame, R. T., Noom, M. C. & Wuite, G. J. L. (2006). Bacterial chromatin organization by H-NS protein unravelled using dual DNA manipulation. *Nature* **444**, 387–390.

De Vlaminck, I. & Dekker, C. (2012). Recent advances in magnetic tweezers. *Annual Review of Biophysics* **41**, 453–472.

De Vlaminck, I., Henighan, T., van Loenhout, M. T. J., Pfeiffer, I., Huijts, J., Kerssemakers, J. W. J., Katan, A. J., van Langen-Suurling, A., van der Drift, E., Wyman, C. & Dekker, C. (2011). Highly parallel magnetic tweezers by targeted DNA tethering. *Nano Letters* **11**, 5489–5493.

De Vlaminck, I., van Loenhout, M. T. J., Zweifel, L., den Blanken, J., Hooning, K., Hage, S., Kerssemakers, J. & Dekker, C. (2012). Mechanism of homology recognition in DNA recombination from dual-molecule experiments. *Molecular Cell* **46**, 616–624.

DiCapua, E., Schnarr, M., Ruigrok, R. W., Lindner, P. & Timmins, P. A. (1990). Complexes of RecA protein in solution. A study by small angle neutron scattering. *Journal of Molecular Biology* **214**, 557–570.

Forget, A. L. & Kowalczykowski, S. C. (2012). Single-molecule imaging of DNA pairing by RecA reveals a three-dimensional homology search. *Nature* **482**, 423–427.

Galletto, R., Amitani, I., Baskin, R. J. & Kowalczykowski, S. C. (2006). Direct observation of individual RecA filaments assembling on single DNA molecules. *Nature* **443**, 875–878.

Gibb, B., Silverstein, T. D., Finkelstein, I. J. & Greene, E. C. (2012). Single-stranded DNA curtains for real-time single-molecule visualization of protein-nucleic acid interactions. *Analytical Chemistry* **84**, 7607–7612.

Gorman, J. & Greene, E. C. (2008). Visualizing one-dimensional diffusion of proteins along DNA. *Nature Structural and Molecular Biology* **15**, 768–774.

Gorman, J., Fazio, T., Wang, F., Wind, S. & Greene, E. C. (2010). Nanofabricated racks of aligned and anchored DNA substrates for single-molecule imaging. *Langmuir: the ACS Journal of Surfaces and Colloids* **26**, 1372–1379.

Gross, P., Laurens, N., Oddershede, L. B., Bockelmann, U., Peterman, E. J. G. & Wuite, G. J. L. (2011). Quantifying how DNA stretches, melts and changes twist under tension. *Nature Physics* **7**, 731–736.

Gupta, R. C., Folta-Stogniew, E., O'Malley, S., Takahashi, M. & Radding, C. M. (1999). Rapid exchange of A:T base pairs is essential for recognition of DNA homology by human Rad51 recombination protein. *Molecular Cell* **4**, 705–714.

Ha, T., Enderle, T., Ogletree, D. F., Chemla, D. S., Selvin, P. R. & Weiss, S. (1996). Probing the interaction between two single molecules: fluorescence resonance energy transfer between a single donor and a single acceptor. *Proceedings of the National Academy of Sciences of the United States of America* **93**, 6264–6268.

Ha, T., Kozlov, A. G. & Lohman, T. M. (2012). Single-molecule views of protein movement on single-stranded DNA. *Annual Review of Biophysics* **41**, 295–319.

Hegner, M., Smith, S. B. & Bustamante, C. (1999). Polymerization and mechanical properties of single RecA-DNA filaments. *Proceedings of the National Academy of Sciences* **96**, 10109–10114.

Heyer, W. -D., Ehmsen, K. T. & Liu, J. (2010). Regulation of homologous recombination in eukaryotes. *Annual Review of Genetics* **44**, 113–139.

Hilario, J., Amitani, I., Baskin, R. J. & Kowalczykowski, S. C. (2009). Direct imaging of human Rad51 nucleoprotein dynamics on individual DNA molecules. *Proceedings of the National Academy of Sciences of the United States of America* **106**, 361–368.

Hoeijmakers, J. H. (2001). Genome maintenance mechanisms for preventing cancer. *Nature* **411**, 366–374.

Holden, S. J., Uphoff, S., Hohlbein, J., Yadin, D., Le Reste, L., Britton, O. J. & Kapanidis, A. N. (2010). Defining the limits of single-molecule FRET resolution in TIRF microscopy. *Biophysical Journal* **99**, 3102–3111.

Holloman, W. K. (2011). Unraveling the mechanism of BRCA2 in homologous recombination. *Nature Structural and Molecular Biology* **18**, 748–754.

Howard-Flanders, P., West, S. C. & Stasiak, A. (1984). Role of RecA protein spiral filaments in genetic recombination. *Nature* **309**, 215–220.

Inoue, K. & Lupski, J. R. (2002). Molecular mechanisms for genomic disorders. *Annual Review of Genomics and Human Genetics* **3**, 199–242.

Jensen, R. B., Carreira, A. & Kowalczykowski, S. C. (2010). Purified human BRCA2 stimulates RAD51-mediated recombination. *Nature* **467**, 678–683.

https://doi.org/10.1017/S0033583513000073 Published online by Cambridge University Press

Joo, C., McKinney, S. A., Nakamura, M., Rasnik, I., Myong, S., Ha, T. (2006). Real-time observation of RecA filament dynamics with single monomer resolution. *Cell* **126**, 515–527.

Kim, K. & Saleh, O. A. (2009). A high-resolution magnetic tweezer for single-molecule measurements. *Nucleic Acids Research* **37**, e136.

Kowalczykowski, S. C., Dixon, D. A., Eggleston, a. K., Lauder, S. D. & Rehrauer, W. M. (1994). Biochemistry of homologous recombination in Escherichia coli. *Microbiological Reviews* **58**, 401–465.

Lipfert, J., Kerssemakers, J. W. J., Jager, T. & Dekker, N. H. (2010). Magnetic torque tweezers: measuring torsional stiffness in DNA and RecA–DNA filaments. *Nature Methods* **7**, 977–980.

Lipfert, J., Wiggin, M., Kerssemakers, J. W. J., Pedaci, F. & Dekker, N. H. (2011). Freely orbiting magnetic tweezers to directly monitor changes in the twist of nucleic acids. *Nature Communications* **2**, 439.

Liu, J., Doty, T., Gibson, B. & Heyer, W. -D. (2010). Human BRCA2 protein promotes RAD51 filament formation on RPA-covered single-stranded DNA. *Nature Structural and Molecular Biology* **17**, 1260–1262.

Mani, A., Braslavsky, I., Arbel-Goren, R. & Stavans, J. (2010). Caught in the act: the lifetime of synaptic intermediates during the search for homology on DNA. *Nucleic Acids Research* **38**, 2036–2043.

Mazin, A. V. & Kowalczykowski, S. C. (1996). The specificity of the secondary DNA binding site of RecA protein defines its role in DNA strand exchange. *Proceedings of the National Academy of Sciences of the United States of America* **93**, 10673–10678.

Mazin, A. V. & Kowalczykowski, S. C. (1998). The function of the secondary DNA-binding site of RecA protein during DNA strand exchange. *EMBO Journal* **17**, 1161–1168.

McKinnon, P. J. & Caldecott, K. W. (2007). DNA strand break repair and human genetic disease. *Annual Review of Genomics and Human Genetics* **8**, 37–55.

McKinney, S. a., Joo, C. & Ha, T. (2006). Analysis of single-molecule FRET trajectories using hidden Markov modeling. *Biophysical Journal* **91**, 1941–1951.

Moffitt, J. R., Chemla, Y. R., Smith, S. B. & Bustamante, C. (2008). Recent advances in optical tweezers. *Annual Review of Biochemistry* **77**, 205–228.

Negrini, S., Gorgoulis, V. G. & Halazonetis, T. D. (2010). Genomic instability–an evolving hallmark of cancer. *Nature Reviews Molecular Cell Biology* **11**, 220–228.

Neuman, K. C. & Block, S. M. (2004). Optical trapping. *Review of Scientific Instruments* **75**, 2787–2809.

Nomme, J., Takizawa, Y., Martinez, S. F., Renodon-Cornière, A., Fleury, F., Weigel, P., Yamamoto, K., Kurumizaka, H., Takahashi, M. (2008). Inhibition of filament formation of human Rad51 protein by a small peptide derived from the BRC-motif of the BRCA2 protein. *Genes to Cells: Devoted to Molecular and Cellular Mechanisms* **13**, 471–481.

Noom, M. C., Van den Broek, B., Van Mameren, J. & Wuite, G. J. L. (2007). Visualizing single DNA-bound proteins using DNA as a scanning probe. *Nature Methods* **4**, 1031–1036.

Pierobon, P., Miné-Hattab, J., Cappello, G., Viovy, J. -L. & Lagomarsino, M. (2010). Separation of time scales in one-dimensional directed nucleation-growth processes. *Physical Review E* **82**, 061904.

Prvost, C. & Takahashi, M. (2003). Geometry of the DNA strands within the RecA nucleofilament: role in homologous recombination. *Quarterly Reviews of Biophysics* **36**, 429–453.

Quake, S. R., Babcock, H. & Chu, S. (1997). The dynamics of partially extended single molecules of DNA. *Nature* **388**, 151–154.

Ragunathan, K., Joo, C. & Ha, T. (2011). Real-time observation of strand exchange reaction with high spatiotemporal resolution. *Structure* (*London, England: 1993*) **19**, 1064–1073.

Reymer, A., Frykholm, K., Morimatsu, K., Takahashi, M. & Nordén, B. (2009). Structure of human Rad51 protein filament from molecular modeling and site-specific linear dichroism spectroscopy. *Proceedings of the National Academy of Sciences of the United States of America* **106**, 13248–13253.

Robertson, R. B., Moses, D. N., Kwon, Y., Chan, P., Chi, P., Klein, H., Sung, P., Greene, E. C. (2009). Structural transitions within human Rad51 nucleoprotein filaments. *Proceedings of the National Academy of Sciences of the United States of America* **106**, 12688–12693.

Roy, R., Hohng, S. & Ha, T. (2008). A practical guide to single-molecule FRET. *Nature Methods* **5**, 507–516.

San Filippo, J., Sung, P. & Klein, H. (2008). Mechanism of eukaryotic homologous recombination. *Annual Review of Biochemistry* **77**, 229–257.

Santoso, Y., Joyce, C. M., Potapova, O., Le Reste, L., Hohlbein, J., Torella, J. P., Grindley, N. D. F., Kapanidis, A. N. (2010). Conformational transitions in DNA polymerase I revealed by single-molecule FRET. *Proceedings of the National Academy of Sciences of the United States of America* **107**, 715–720.

Shaevitz, J. W., Abbondanzieri, E. A., Landick, R. & Block, S. M. (2003). Backtracking by single RNA polymerase molecules observed at near-base-pair resolution. *Nature* **426**, 684–687.

Smith, S., Finzi, L. & Bustamante, C. (1992). Direct mechanical measurements of the elasticity of single DNA molecules by using magnetic beads. *Science* **258**, 1122–1126.

Strick, T. R., Allemand, J. -F. F., Bensimon, D., Bensimon, A. & Croquette, V. (1996). The Elasticity of a Single Supercoiled DNA Molecule. *Science* **271**, 1835–1837.

https://doi.org/10.1017/S0033583513000073 Published online by Cambridge University Press

Takahashi, M. (1989). Analysis of DNA-RecA protein interactions involving the protein self-association reaction. *Journal of Biological Chemistry* **264**, 288–295.

Tombline, G. & Fishel, R. (2002). Biochemical characterization of the human RAD51 protein. I. ATP hydrolysis. *Journal of Biological Chemistry* **277**, 14417–14425.

Van der Heijden, T. & Dekker, C. (2008). Monte Carlo simulations of protein assembly, disassembly, and linear motion on DNA. *Biophysical Journal* **95**, 4560–4569.

van der Heijden, T., Seidel, R., Modesti, M., Kanaar, R., Wyman, C., Dekker, C. (2007). Real-time assembly and disassembly of human RAD51 filaments on individual DNA molecules. *Nucleic Acids Research* **35**, 5646–5657.

van der Heijden, T., Modesti, M., Hage, S., Kanaar, R., Wyman, C., Dekker, C. (2008). Homologous recombination in real time: DNA strand exchange by RecA. *Molecular Cell* **30**, 530–538.

Van Loenhout, M. T. J., Van der Heijden, T., Kanaar, R., Wyman, C. & Dekker, C. (2009). Dynamics of RecA filaments on single-stranded DNA. *Nucleic Acids Research* **37**, 4089–4099.

van Mameren, J., Modesti, M., Kanaar, R., Wyman, C., Peterman, E. J. G., Wuite, G. J. L. (2009a). Counting RAD51 proteins disassembling from nucleoprotein filaments under tension. *Nature* **457**, 745–748.

van Mameren, J., Gross, P., Farge, G., Hooijman, P., Modesti, M., Falkenberg, M., Wuite, G. J. L., Peterman, E. J. G. (2009b). Unraveling the structure of DNA during overstretching by using multicolor, single-molecule fluorescence imaging. *Proceedings of the National Academy of Sciences of the United States of America* **106**, 18231–18236.

Wold, M. S. (1997). Replication protein A: a heterotrimeric, single-stranded DNA-binding protein required for eukaryotic DNA metabolism. *Annual Review of Biochemistry* **66**, 61–92.

Wyman, C. & Kanaar, R. (2006). DNA double-strand break repair: all's well that ends well. *Annual Review of Genetics* **40**, 363–383.

Xiao, J., Lee, A. M. & Singleton, S. F. (2006). Direct evaluation of a kinetic model for RecA-mediated DNA-strand exchange: the importance of nucleic acid dynamics and entropy during homologous genetic recombination. *Chembiochem: a European Journal of Chemical Biology* **7**, 1265–1278.

Yodh, J. G., Schlierf, M. & Ha, T. (2010). Insight into helicase mechanism and function revealed through single-molecule approaches.

Yu, X., Jacobs, S. a., West, S. C., Ogawa, T. & Egelman, E. H. (2001). Domain structure and dynamics in the helical filaments formed by RecA and Rad51 on DNA. *Proceedings of the National Academy of Sciences of the United States of America* **98**, 8419–8424.

https://doi.org/10.1017/S0033583513000073 Published online by Cambridge University Press